Dynamics of Brittle Fracture with Variable Elasticity

Farid F. Abraham

IBM Research Division, Almaden Research Center, 650 Harry Road, San Jose, California 95120-6099

(Received 3 January 1996)

Simulations show that brittle cracks approach six-tenths the Rayleigh speed and follow the highest surface energy path. Using an interatomic potential recently developed by J. P. Sethna, we find that the crack's limiting speed now approaches the theoretical prediction of the Rayleigh speed, but the crack path is still associated with greatest elastic stiffness and surface energy. We conclude that the crack's dynamics is governed by the anisotropic mean-field elasticity associated with large strains ($\geq 7\%$). [S0031-9007(96)00740-5]

PACS numbers: 62.20.Mk

With the advent of scalable parallel computers, classical molecular dynamics has become a very powerful tool for providing immediate insights into the nature of fracture dynamics [1,2]. We have studied rapid brittle fracture of two-dimensional notched solids under tension using 10^6 atom systems. Similar to recent experiments [3], our initial interest was to study the instability dynamics of failure under "mode one" loading. From the computer simulations [1], an explanation for the limiting speed of the crack being significantly less than the theoretical limit became apparent. Also many microscopic processes governing the fracture process were identified, such as the presence of dislocation emission when the crack becomes unstable.

However, we also learned from simulations using the simple Lennard-Jones potential that the crack favors a path along the highest surface energy face [4]; the surface energy for a given crystal face (a line for a 2D solid) is calculated by counting the number of broken bonds per unit length for the relaxed, zero temperature solid along a chosen direction. This is contrary to conventional wisdom which would identify the lowest energy surface as the cleavage direction. Because the elastic constants are profoundly anisotropic for large strains, we questioned whether this elastic anisotropy was the reason. Sethna has recently modified the Lennard-Jones potential which gives an isotropic modulus with an anomalous increase up to very large strains ($<6\%$), though still short of the maximum tip strain [5]. We find similar path behavior for the brittle fracture, but with an enhanced limiting crack velocity approximating the Rayleigh speed. We propose an explanation for crack speed approaching the theoretical limit based on the anisotropic mean-field elasticity associated with large strains ($\geq 7\%$) and the role of elastic fluctuations in the anisotropic medium. We now discuss the interatomic potentials, their elasticity, the model system for the fracture simulations, the simulation results, and our conclusions.

The interatomic forces are treated as central forces, modeled as a combination of a Lennard-Jones (LJ) 12:6 with a spline cutoff [6]. The LJ 12:6 part is simply

$$\phi_{\mathrm{LJ}}(r) = 4\epsilon[(\sigma/r)^{12} - (\sigma/r)^{6}],$$

where ϵ is the LJ well depth and σ is where the potential goes through zero. We express quantities in terms of reduced units; lengths are scaled by σ, energies by ϵ. As discussed previously [6], this model potential can be used to represent a "brittle" material. In Fig. 1(a), we present the Young's modulus for a 2D triangular lattice of Lennard-Jones atoms for two orthogonal directions of the applied strain. The modulus is calculated by expanding the crystal uniformly in a chosen direction and relaxing it in the orthogonal direction by an amount which minimizes the total potential energy (at zero temperature). The equilibrium contraction determines the Poisson ratio for the applied strain. The resulting stress is calculated using the viral expression for the pressure tensor. The stress as a function of strain determines the Young's modulus. We have strained the 2D solid in two orthogonal directions; the "soft" direction corresponds to a row of atoms along that direction being spaced by the lattice constant a, and the "stiff" (orthogonal) direction is where these same rows are separated in the perpendicular direction by $\sqrt{3}/2a$ [see Fig. 1(a)]. Soft denotes the smallest Young's modulus, and stiff denotes the largest modulus. The triangular lattice properties under large deformations are not isotropic: rotating by 90° will exchange the points with the sides of the hexagons, and directional dependences on lattice structure can be reflected in materials' properties, which is the case for large strains. We also note that the soft direction is the weak direction, failing at a strain of $\sim 13\%$ in contrast to the stiff direction that is the strong direction that has a failing strain of $\sim 19\%$.

By a suitable choice of the interatomic potential, one can make the long-wavelength behavior substantially more isotropic by forcing the first few nonlinear elastic coefficients to be isotropic [5]. It should be mentioned that the simple harmonic potential does not give elastic isotropy beyond a very modest strain of 1%. The analysis is quite simple if one assumes only nearest-neighbor forces. Equating the energy for equivalent strains along

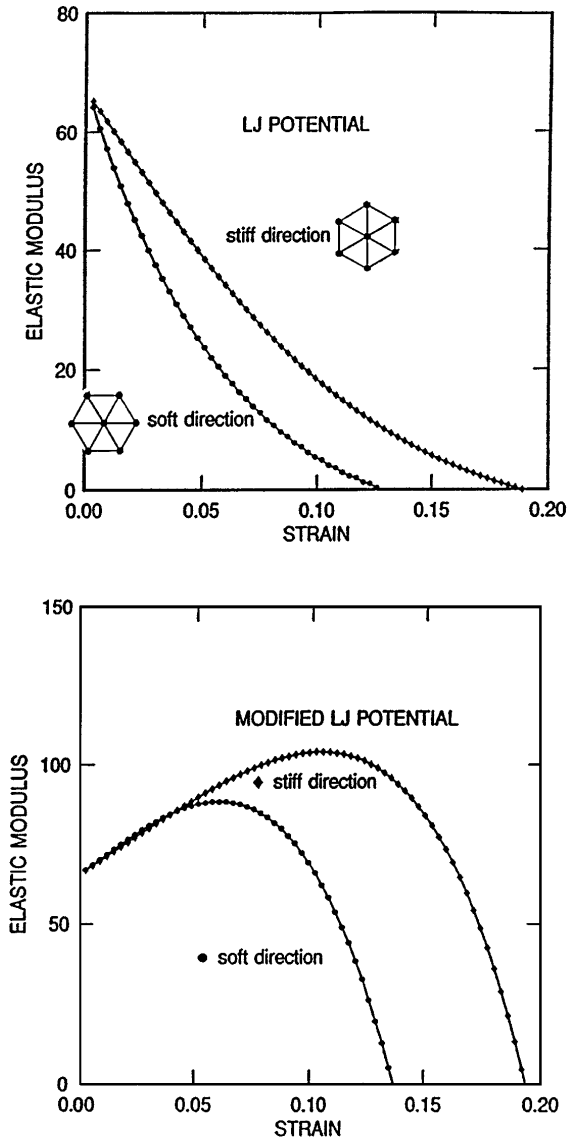

FIG. 1. (a) Dependence of Young's modulus on mode I strain for a 2D LJ crystal, and (b) for a 2D "modified" LJ crystal, where the triangular lattice is stretched in the soft and stiff directions, respectively. The lattice clusters inserted in (a) depict the lattice orientation giving soft and stiff moduli for an imposed horizontal strain.

the xx and xy directions to third order in the strains leads to the constraint

$$V'''(a) = (3/a)V''(a).$$

There is one more independent third-order nonlinear elastic constant for a hexagonal material than for an isotropic material, so this constraint is the only one: any pair potential satisfying this will be isotropic to third order. Similarly, to fourth order the constraint

$$V''''(a) = (3/a)\,V''(a)$$

produces an isotropic potential. The cubic and quadratic terms are added to the Lennard-Jones pair potential, to satisfy these two constraints,

$$V_{\text{add}}(r) = 288(r/a - 1)^3 - 1104(r/a - 1)^4.$$

This potential reaches a maximum at 1.354 96, where (coincidentally) its value is quite close to zero ($-0.001\,227\,15$). The potential is cut off at this radius, which is below the second-neighbor distance. From Fig. 1(b), we see that the new modified pair potential gives an isotropic elastic solid for strains up to 6%, expanding the strain range for isotropy significantly. Also, the modulus increases in this region, meaning that the solid becomes stiffer upon expansion. However, beyond a strain of $\epsilon_{\max} \sim 6\%$, the moduli for the two orthogonal directions separate and retain their original orientational dependence for being stiff and soft. Similar to the LJ solid, the soft direction fails at a strain of $\sim$14%, and the stiff direction fails at $\sim$19%. However, the magnitudes of the moduli in the anisotropic region for the LJ solid and the modified LJ (MLJ) solid have entirely different dependences; e.g., at the failure points for the soft direction of the two solids, the stiff modulus for the LJ solid is very small, while the stiff modulus for the modified LJ solid is approximately at its maximum. These are features that we will return to when we discuss the results of the simulation experiments. Also, the surface energy for the LJ solid and the MLJ solid are equal for a chosen crystal direction since the two potentials are identical for zero strain.

We now consider the fracture simulation model using these potentials. The system is a 2D rectangular slab of atoms with L atoms on a side where $L = 1424$ for the $\sim 2 \times 10^6$ atom system. The slab is initialized at a reduced temperature of 0.000 01. A notch of 60 lattice spacings is cut midway along the lower horizontal slab boundary, and an outward strain rate $\dot{\varepsilon}_x$ is imposed on the outermost columns of atoms defining the opposing vertical faces of the slab. A linear velocity gradient is established across the slab, and an increasing lateral strain with time occurs in the solid slab with an applied strain rate of $\dot{\varepsilon}_x = 0.0001$. With this choice, the solid fails at the notch tip when the solid has been stretched by $\sim$1.5%. At the onset of crack motion, the imposed strain rate remains constant (experiment 1) or is set to zero (experiment 2), and the simulation is continued until the growing crack has traversed the total length of the slab. Both experiments give the same dynamical behavior, and we choose to report on the first type of experiment.

As mentioned in the introduction, we have learned that the overall features of the fracture simulations on the 2D LJ solid depended on the crystal orientation (Fig. 2). In our earliest experiments [1], the notch is pointed in the stiff direction. We observed that the crack's net motion remains in that direction, with oscillations about that direction. We also did the same fracture simulation but rotated the notch by 90° from the original orientation, or in the soft direction. This direction is termed the cleavage plane (line) since the created surface by fracture has the lowest energy and is believed to be the favored

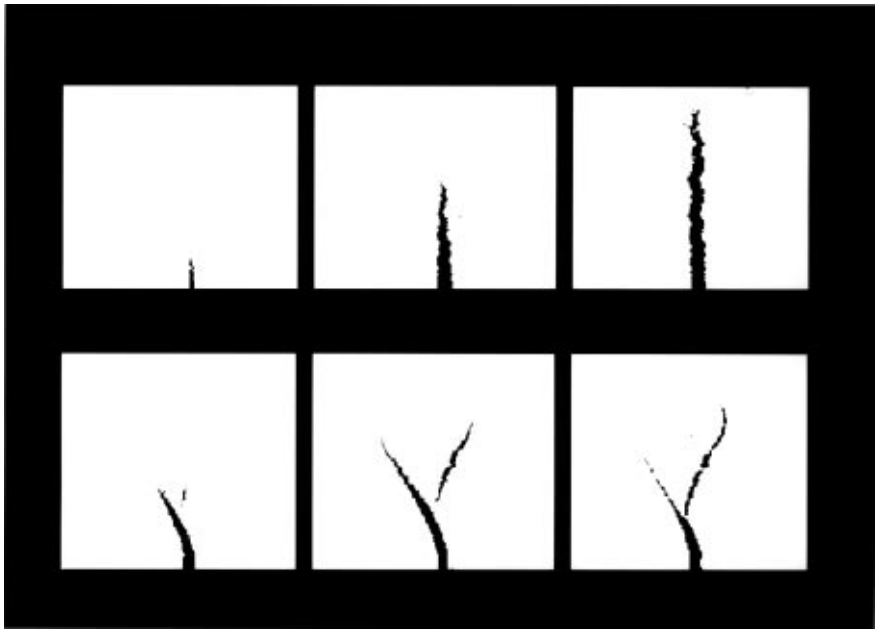

FIG. 2. Past simulations using the original LJ potential (see Ref. [4]); a black and white rendering is used to show the time evolution of the propagating crack through the solid slab. The time sequence goes from left to right. The top row is for the crack initially moving in the stiff direction, and the bottom row is for the crack initially moving in the soft direction. The system is $\sim 5 \times 10^5$ atoms.

direction for fracture. As a function of crystal direction, the surface energy changes by 15%. However, in this orientation, the crack does not proceed along this cleavage line, but turns toward the orthogonal direction, then branches. Because of the hexagonal crystal symmetry, this branched direction, which is 30° from the cleavage direction, corresponds to a stiff axis; that is to say, the crack path favors the stiff direction. The anisotropy in the elasticity for all

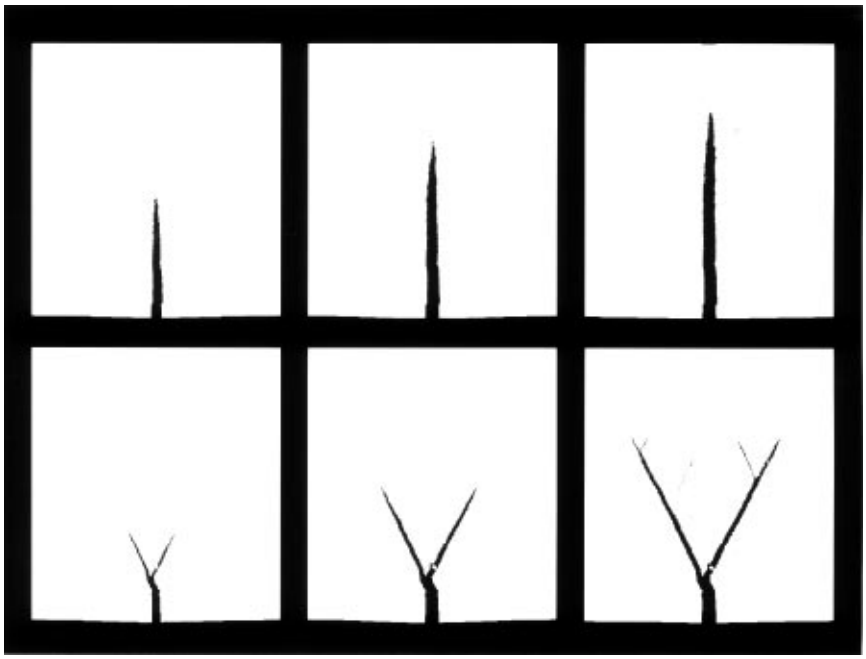

FIG. 3. Black and white rendering of the time evolution of the propagating crack using the modified LJ interatomic potential. The time sequence goes from left to right. The top row is for initial motion in the stiff direction and for a slab with dimensions 1233 atoms by 1644 atoms. The time interval between the first and second images is 72 and between the second and third images is 43.2 (reduced units). The bottom row is for initial motion in the soft direction and for a slab with dimensions 1424 atoms by 1424 atoms. The time interval between the each consecutive image is 72.

strains [Fig. 1(a)] led us to suspect that this was the origin for this particular fracture behavior. This is consistent with a continuum analysis of Gao [7].

The same two simulations with the modified LJ potential are presented in Fig. 3. Similar path behavior exists between the LJ and modified LJ solids (Figs. 2 and 3), even though the solids are elastically quite different (Fig. 1). Considering $0 \leq \epsilon \leq 6\%$, the LJ modulus is anisotropic and a monotonically decreasing function of strain while the MLJ modulus is isotropic and increases. Hence, we conclude that the elasticity of the solids with strains up to 6% does not play a governing role for the crack path in brittle fracture. For $6\% \leq \epsilon \leq 20\%$, the common feature of the LJ and MLJ elastic moduli is their failure points: the soft moduli fail at $\sim$13%, and the stiff moduli fail at $\sim$19%. This suggests a simple picture for the crack path behavior; the crack path follows the stiff direction because the bonds fail at a much lower strain. If the crack is initially moving in the stiff direction, it will "stay" in that direction. Otherwise, a crack initialized in the soft direction will eventually "branch" by $\pm 30°$, the branch can be a single crack or a multicrack with a vertex at the point of branching. If the branch is a single crack, the material will "tear" in the symmetrically opposite side because of the created mixed mode (mode I and mode II) asymmetry. This is vividly seen in Fig. 2.

The anisotropic elasticity plays a major role in the direction of the crack path, and it also plays a very important role in the fluctuation dynamics of the crack tip moving along the stiff direction. For the Lennard-Jones solid, the maximum tip speed is approximately six-tenths of the theoretically predicted limit, or the Rayleigh speed. From Fig. 2(a) [1] for the LJ solid, we see the onset of a crack instability beginning as a roughening of the created surfaces which quickly grows into a pronounced zigzag or wavy tip motion. The oscillating zigzag motion of the crack tip results in the apparent "forward" crack speed being significantly less than theoretical prediction (for details see Ref. [1]). However, for the MLJ solid, the maximum tip velocity approaches the theoretically predicted limit; i.e., it is about 0.9 times the Rayleigh sound speed. This is because the crack tip is not dramatically zigzagging about the forward, and its "apparent" forward speed is its actual forward speed. Why are there significant directional deviations about the forward motion for the LJ solid and not for the MLJ solid? We recall from Fig. 1 that at the failure points for the soft direction of the two solids, the stiff modulus for the LJ solid is very small, while the stiff modulus for the modified LJ solid is almost a maximum. Hence, for the LJ solid, asymmetrical strain fluctuations about the forward direction of motion could lead to failure along the stiff direction because of the significant elastic softening in that direction. Such is not the case for the MLJ solid; while failing in one direction, it is near its highest strength at the next nearest lattice symmetry direction given by a 30° rotation from the forward direction. However, there is still a surface roughening of the MLJ solid that begins at about one-third of the Rayleigh speed.

In summary, we have found that there are two distinct directions in a triangular LJ solid, a stiff direction along which the yield strain is large and a soft direction along which the yield strain is smaller. A crack propagates more stably along the stiff direction even though it creates a surface of higher energy. In other words, the crack does not dynamically choose the low-energy cleavage direction as is generally supposed in conventional fracture theory. While maintaining the same surface energy, the MLJ potential substantially increases the difference between stiff and soft directions at large strains in such a way as to enhance the stability of cracks moving in the stiff direction. Hence, it is the detailed stresses near the crack tip, rather than the surface energy, that control directional stability of fracture.

Jim Sethna developed the modified potential at the Aspen Center of Physics. I am indebted to him for his contribution. I am grateful for discussions with Professor H. Gao, Applied Mechanics at Stanford. I acknowledge a grant at the Cornell Theory Center, which receives funding from the NSF, New York State, ARPA, the National Center for Research Resources at NIH, IBM, and members of the Corporate Research Institute.

[1] F. F. Abraham, D. Brodbeck, R. Rafey, and W. E. Rudge, Phys. Rev. Lett. **73**, 272 (1994).
[2] A. Nakano, R. K. Kalia, and P. Vashishta, Phys. Rev. Lett. **75**, 3138 (1995).
[3] J. Fineberg, S. P. Gross, M. Marder, and H. L. Swinney, Phys. Rev. Lett. **67**, 457 (1991); Phys. Rev. B **45**, 5146 (1992); S. P. Gross, J. Fineberg, M. Marder, W. D. McCormick, and H. L. Swinney, Phys. Rev. Lett. **71**, 3162 (1993).
[4] F. F. Abraham, in *Computer Simulation in Materials Science*, edited by H. O. K. Kirchner, and V. Pontikis, NATO ASI (Kluwer Publishing, The Netherlands, 1996).
[5] J. P. Sethna, (private communication).
[6] N. J. Wagner, B. L. Holian, and A. F. Voter, Phys. Rev. A **45**, 8457 (1992).
[7] H. Gao, Int. J. Solids Struct. **29**, 947 (1992).